magnetic equator, $J_\perp$ can be determined with the low-energy telescope which is oriented nearly perpendicular to the magnetic field.

The results in Table 2 show that the phase space density $J_\perp/B$ at constant M decreases by a factor of ~ 10 between 12 and 10 R_J. The positive radial gradient in $J_\perp/B$ is a direct indication that the anomalous oxygen (and probably the sodium and sulfur as well) is diffusing inward. In the mid-magnetosphere ($B \sim 10^{-4}$ G), these particles would have energies $E \gtrsim 240$ keV per nucleon. Substantial intensities of oxygen and sulfur ions at these energies were detected by both Voyager 1 and Voyager 2 in the outer and middle magnetosphere, but with lower intensities during the Voyager 2 encounter (*4, 12*).

The spectra of the oxygen ions with energies between 4.2 and 14 MeV per nucleon between 10 and 25 R_J can be well represented by $dJ/dE \sim E^{-\gamma}$, with $\gamma = 4.5 \pm 0.5$. The value of the spectral index γ changes little in the region from 10 to 25 R_J and is similar to that observed near 220 keV per nucleon in the outer magnetosphere on Voyager 1 (*4*). A radial diffusion process would preserve such a power law spectrum, provided that the loss processes were energy-independent.

The source of anomalous oxygen and sulfur in the outer magnetosphere or in the solar wind may be similar to that proposed by Eviatar *et al.* (*14*), who suggested that charge exchange between corotating sodium ions and neutral atoms in the Io sodium cloud could result in fast neutral sodium atoms which escape from Io's orbit and populate the outer magnetosphere and solar wind. The reionization of the sodium atoms was proposed as the source of sodium ions, which would then be subsequently accelerated through inward radial diffusion. Such high-energy sodium nuclei were observed by Voyager 1 (see Table 1). The Voyager 2 results suggest a similar source for low-energy oxygen and sulfur ions in the outer regions based on the reionization of fast neutral oxygen and sulfur atoms which may have been produced from the corotating oxygen, sulfur, and sulfur dioxide ions in the Io torus (*15*).

R. E. VOGT
A. C. CUMMINGS
T. L. GARRARD
N. GEHRELS, E. C. STONE
California Institute of Technology, Pasadena 91125
J. H. TRAINOR, A. W. SCHARDT
T. F. CONLON, F. B. MCDONALD
NASA Goddard Space Flight Center, Greenbelt, Maryland 20771

References and Notes

1. R. E. Vogt *et al.*, *Science* **204**, 1003 (1979).
2. See relevant articles in *Jupiter*, T. Gehrels, Ed. (Univ. of Arizona Press, Tucson, 1976).
3. C. F. Kennel and F. V. Coroniti, *Annu. Rev. Astron. Astrophys.* **15**, 389 (1977).
4. S. M. Krimigis *et al.*, *Science* **204**, 998 (1979).
5. F. B. McDonald, A. W. Schardt, J. H. Trainor, *J. Geophys. Res.* **84**, 2579 (1979).
6. N. F. Ness *et al.*, *Science* **206**, 966 (1979).
7. V. M. Vasyliunas, *Geophys. Res. Lett.* **2**, 87 (1975); A. J. Dessler, *ibid.* **5**, 65 (1978).
8. E. C. Stone and A. L. Lane, *Science* **206**, 925 (1979).
9. Jet Propulsion Laboratory trajectory calculation based on model D4 of E. J. Smith, L. Davis, Jr., and D. E. Jones, in (*2*), p. 788.
10. T. G. Northrop, C. K. Goertz, M. F. Thomsen, *J. Geophys. Res.* **79**, 3579 (1974); M. G. Kivelson, P. J. Coleman, Jr., L. Froidevaux, R. L. Rosenberg, *ibid.* **83**, 4823 (1978).
11. D. L. Chenette, T. F. Conlon, J. A. Simpson, *ibid.* **79**, 3551 (1974); W. Fillius and P. Knickerbocker, *J. Geophys. Res.*, in press.
12. S. M. Krimigis *et al.*, *Science* **206**, 977 (1979).
13. See, for example, M. Shulz and L. J. Lanzerotti, *Particle Diffusion in the Radiation Belts* (Springer-Verlag, New York, 1974).
14. A. Eviatar, Y. Mekler, F. V. Coroniti, *Astrophys. J.* **205**, 622 (1976).
15. A. L. Broadfoot *et al.*, *Science* **204**, 979 (1979); H. S. Bridge *et al.*, *ibid.*, p. 987.

16. We thank N. Ness and his colleagues on the Voyager magnetometer team for providing the magnetic field data used in this analysis.
17. We thank the Voyager Project and the enthusiastic staff of our laboratories at the California Institute of Technology (Caltech) and the Goddard Space Flight Center (GSFC) for splendid support. Special thanks go to W. Althouse and J. Povlis (Caltech), J. Broomhall and J. Zipse of Computer Sciences Corporation, W. Davis, H. Domchick, and D. Stilwell (GSFC), and E. Franzgrote (Jet Propulsion Laboratory) who had major responsibilities. The team was greatly assisted in the near-real-time data analysis by the following Caltech undergraduates: T. Cowan, J. Ennis, D. Gordon, H. King, and especially T. Van Eck who wrote several special computer programs. Supported by NASA under contracts NAS 7-100 and NGR 05-002-160.

26 September 1979

Plasma Wave Observations Near Jupiter: Initial Results from Voyager 2

Abstract. *This report provides an initial survey of results from the plasma wave instrument on the Voyager 2 spacecraft, which flew by Jupiter on 9 July 1979. Measurements made during the approach to the planet show that low-frequency radio emissions from Jupiter have a strong latitudinal dependence, with a sharply defined shadow zone near the equatorial plane. At the magnetopause a new type of broadband electric field turbulence was detected, and strong electrostatic emissions near the upper hybrid resonance frequency were discovered near the low-frequency cutoff of the continuum radiation. Strong whistler-mode turbulence was again detected in the inner magnetosphere, although in this case extending out to substantially larger radial distances than for Voyager 1. In the predawn tail region, continuum radiation was observed extending down to extremely low frequencies, ~ 30 hertz, an indication that the spacecraft was entering a region of very low density, $\sim 1.0 \times 10^{-5}$ per cubic centimeter, possibly similar to the lobes of Earth's magnetotail.*

The Voyager 2 flyby of Jupiter, which occurred in July 1979, provided the second opportunity to study plasma waves in the vicinity of Jupiter (the first measurements were made by Voyager 1, which flew by Jupiter in March 1979). Because of the somewhat different trajectory and plasma conditions at Jupiter, the Voyager 2 mission provided new perspectives for analyzing many of the phenomena detected by Voyager 1 and also revealed the presence of several new types of plasma waves. For a survey of the Voyager 1 plasma wave observations at Jupiter, see Scarf *et al.* (*1*). Starting about 6 months before the closest approach of Voyager 2, intense radio emissions from Jupiter were detected by the Voyager 2 plasma wave instrument at kilometric wavelengths. Closer to the magnetosphere, sporadic bursts of electron plasma oscillations and ion acoustic waves were observed upstream of the bow shock for several weeks. Between about 99 and 62 Jupiter radii (R_J) a total of five crossings of the bow shock and three crossings of the magnetopause were identified in the plasma wave data. At the magnetopause, a new type of electrostatic noise was observed with characteristics similar to those of Earth's magnetopause. Within the magnetosphere continuum radiation trapped in the magnetospheric cavity, electrostatic waves at half-integral harmonics of the electron gyrofrequency, narrowband emissions at the upper hybrid resonance frequency, and whistler-mode chorus and hiss emissions were detected. On the outbound leg through the predawn tail region, strong low-frequency bursts of continuum radiation, modulated by the rotation of Jupiter, were observed; these observations indicated that the spacecraft entered regions of extremely low plasma density, $\sim 1.0 \times 10^{-5}$ cm^{-3}, apparently similar to the tail lobes of Earth's magnetosphere. We present here a survey of the initial results from the Voyager 2 plasma wave instrument, with emphasis on the new observations and comparisons with the Voyager 1 results. The data base for the present discussion starts with the first detection of radio emissions from Jupiter about 6 months before closest approach and ends

0036-8075/79/1123-0987$00.75/0

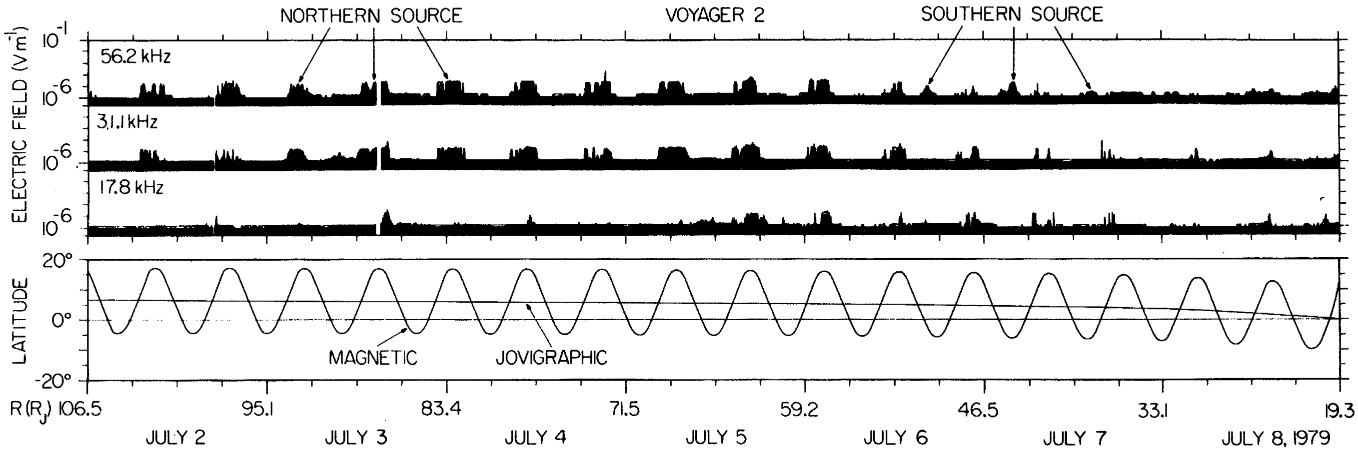

Fig. 1. Observations of Jovian kilometric radiation, showing the regular 10-hour modulation due to Jupiter's rotation. The maximum intensity occurs when the north magnetic pole is tipped toward the spacecraft, an indication of a northern hemisphere source. A transition to viewing the southern hemisphere source can be seen on 7 July, as the spacecraft approaches the equatorial plane.

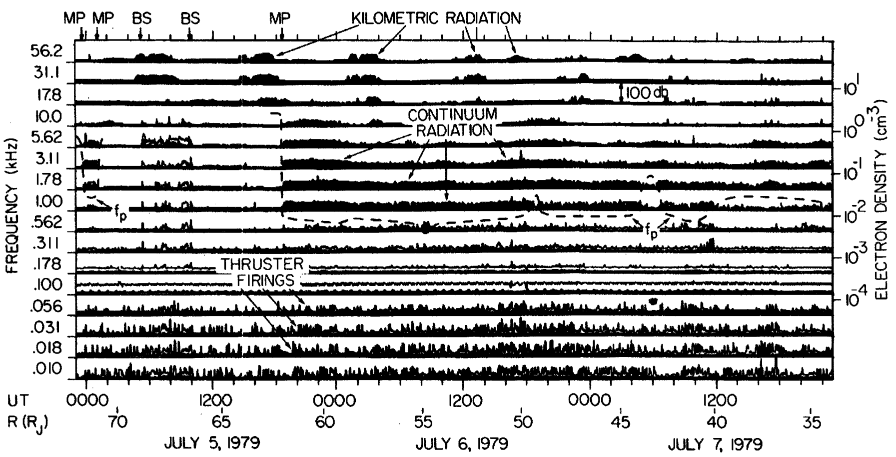

Fig. 2. The inbound pass through the outer regions of the magnetosphere, showing the electromagnetic continuum radiation trapped in the low-density cavity inside the magnetosphere. The low-frequency cutoff of the continuum radiation at the plasma frequency, f_p, provides a direct measurement of the electron density, as indicated by the dashed line.

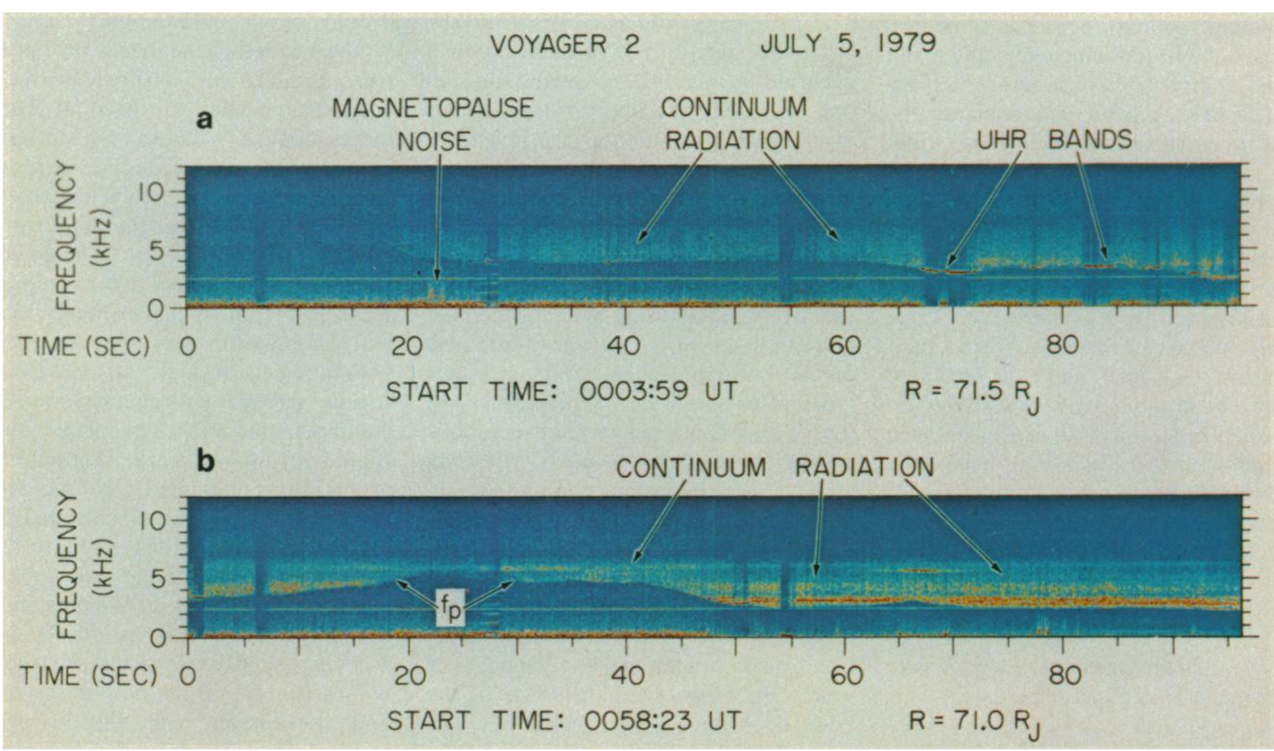

Fig. 3. (a) A wideband color spectrogram showing an intense burst of electric field noise at the magnetopause and narrowband upper hybrid resonance (*UHR*) emissions near the low-frequency cutoff of the continuum radiation. The intensity increases from blue to red, with a total dynamic range of about 20 dB. (b) A spectrogram showing banded structure in the continuum radiation and large variations in the plasma density, as indicated by f_p, on a time scale of only a few seconds.

about 2 weeks after closest approach.

The Voyager plasma wave instruments have been described by Scarf and Gurnett (2). The plasma wave sensor consists of a balanced electric dipole antenna with an effective length of 7 m. The signals from the antenna are processed by a 16-channel spectrum analyzer (10 Hz to 56 kHz) and by a wideband receiver which provides detailed wave-form measurements over the frequency range from 50 Hz to 12 kHz. The Voyager 2 plasma wave instrument operated perfectly throughout the encounter. The only anomaly which affects the data interpretation occurred shortly after launch when a failure in the spacecraft data system caused a distortion and shift in the calibration curve for the upper eight channels of the spectrum analyzers. A new calibration curve for these channels has been reconstructed on the basis of a ground simulation of the failure and appears to give good results. However, since a reconstructed calibration curve is used, one should exercise some caution when using electric field strengths from the upper eight channels of the spectrum analyzer.

Starting in about November 1978, the plasma wave instrument began detecting radio emissions from Jupiter in the 10-Hz to 56-kHz channels. These same radio emissions were also detected by Voyager 1 (1, 3) and will be referred to as Jovian kilometric radiation, since the wavelengths are typically in the kilometer range. The Voyager 2 kilometric radiation observations differ markedly from the Voyager 1 observations in that the radiation is significantly more intense, and shows a much more regular 10-hour modulation due to Jupiter's rotation (Fig. 1). The maximum intensities occur when the spacecraft is at the highest magnetic latitude; this result suggests that the source is in the northern hemisphere. The increased intensity and more regular modulation are believed to be due to the fact that Voyager 2 approached Jupiter at a latitude about 4° higher than Voyager 1. Evidently the radiation pattern of the Jovian kilometric radiation has a strong latitudinal dependence, with a narrow shadow zone near the magnetic equatorial plane.

When the Voyager 2 spacecraft entered the low-density cavity inside the magnetosphere, electromagnetic continuum radiation trapped within the magnetosphere was detected and was found to have characteristics similar to those observed on Voyager 1. Three magnetopause crossings occurred on the inbound pass, at about 0003, 0100, and 1845 UT on 5 July. These magnetopause cross-

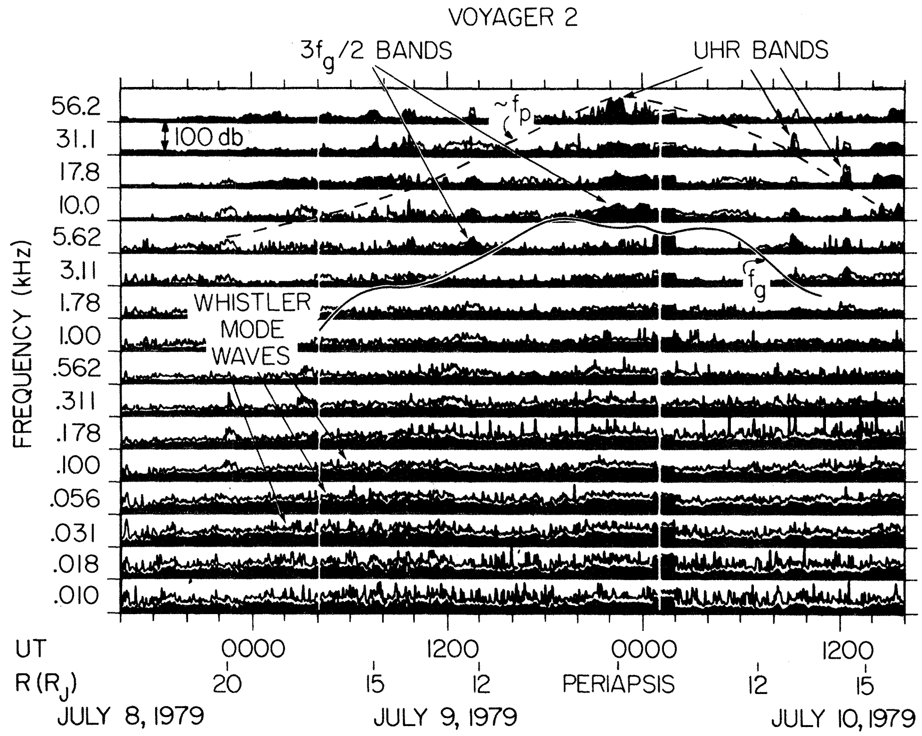

Fig. 4. Plasma wave electric field intensity near closest approach. The electron gyrofrequency profile, f_g, was determined from the magnetometer instrument, and the electron plasma frequency profile is based on our (tentative) identification of emissions at the upper hybrid resonance (*UHR*) frequency. The broadband burst of noise from about 0040 to 0155 UT on 10 July is caused by firing of the trajectory correction thrusters.

ings, labeled MP, and the associated continuum radiation are shown in Fig. 2. The low-frequency cutoff of the continuum radiation is at the local electron plasma frequency (4), $f_p = 9(N)^{1/2}$ kHz, which provides a direct measure of the electron density, N, per cubic centimeter. The approximate density profile in the outer regions of the magnetosphere is shown by the dashed line in Fig. 2. The density decreases from about 2.0 cm^{-3} in the magnetosheath to about 5×10^{-3} cm^{-3} inside the magnetosphere.

Significant new results on the structure of the magnetopause and the origin of the continuum radiation were obtained from the wideband wave-form measurements. Color-coded frequency-time spectrograms of the signals detected near the first and second magnetopause crossings at about 0003 and 0100 UT on 5 July are shown in Fig. 3. The decreasing plasma density at the first magnetopause crossing, as indicated by the continuum radiation cutoff, is clearly evident at about 24 seconds (Fig. 3a). A brief broadband burst of electric field noise extending up to about 2 kHz occurs near the steep density gradient at the magnetopause. This broadband electric field turbulence is very similar to the electric field turbulence that has recently been discovered at Earth's magnetopause (5) and may play an important role in the diffusion and transport of particles across the magnetopause boundary layer.

Later in this same spectrogram, at about 69 seconds and again at about 84 seconds, a series of intense narrowband emissions occurs near the low-frequency cutoff of the continuum radiation. The frequency variation of these intense narrowband emissions is not continuous but consists of a series of discrete steps. Initial comparisons with the magnetic field data (6) indicate that the frequency spacing between the emission lines is the electron gyrofrequency, f_g. Although the emissions occur near f_p, our preliminary interpretation is that these emissions occur when the upper hybrid resonance frequency, $f_{UHR} = (f_p^2 + f_g^2)^{1/2}$, is equal to a half-integral harmonic of f_g, $f_{UHR} = (n + 1/2)f_g$. Intense electrostatic waves of this type, propagating perpendicular to the magnetic field, are frequently observed in Earth's magnetosphere (7). The significance of these narrowband electrostatic emissions is that these waves may be the source of the continuum radiation by means of a nonlinear coupling mechanism. Evidence of such a coupling process can be seen in the continuum radiation spectrum, which frequently shows ill-defined lines and discrete features, such as from about 50 to 96 seconds (Fig. 3b). Figure 3b also shows rather remarkable short-time-scale variations in the cutoff frequency

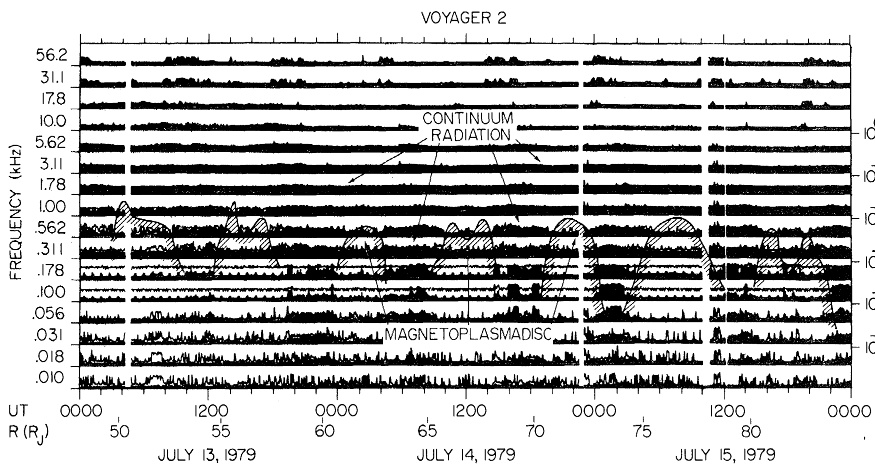

Fig. 5. The plasma wave electric field observations during the outbound pass through the predawn tail region. The continuum radiation cutoff provides a clear identification of the magnetoplasmadisc which was encountered with a regular 10-hour periodicity. Outside of the magnetoplasmadisc, the electron densities are often extremely low, $< 1 \times 10^{-5}$ cm^{-3}; these low values indicate entry into a low-density region, possibly similar to the tail lobes of Earth's magnetosphere.

of the continuum radiation, such as from about 20 to 40 seconds, in which the electron density varies by more than a factor of 4 in 20 seconds. The outer region of the magnetosphere on the dayside of Jupiter often has substantial small-scale density variations, with densities ranging from about 3×10^{-3} to 1×10^{-2} cm^{-3} (see Fig. 2).

Within the inner regions of the magnetosphere, whistler-mode waves resembling chorus and hiss were again detected by Voyager 2. In contrast to Voyager 1, which detected strong whistler-mode emissions only inside of 10 R_J, the whistler-mode emissions detected by Voyager 2 extended over a much broader region of the magnetosphere, out to beyond 20 R_J. The first detection of whistler-mode emissions occurred at about 1830 UT on 8 July, at a radial distance of about 22.5 R_J. These emissions can be seen in the 10- to 100-Hz channels of Fig. 4, gradually increasing in intensity and extending to higher frequencies as the spacecraft approaches Jupiter. On the outbound pass, the whistler-mode emissions continue with sporadic intensity variations out to about 25 R_J. At closest approach the maximum electric field intensities are about 0.1 to 0.2 mV m^{-1}, which are comparable to the maximum electric field intensities observed by Voyager 1 at the same radial distance. The much broader spatial extent of the whistler-mode emissions on Voyager 2 is apparently an indication of a substantial change in the plasma distribution in the inner magnetosphere as compared to the case for Voyager 1. As discussed by Ness *et al.* (*6*), the magnetic field profile shows large depressions compared to the internal field model, which indicates a high-pressure plasma distribution in the region where the whistler-mode emissions were observed.

Other plasma wave emissions identified in the inner region of the magnetosphere include intense electrostatic emissions near half-integral harmonics of the electron gyrofrequency, $3f_g/2$, $5f_g/2$, and intense narrowband emissions at f_{UHR}. These emissions can be seen at about 1330 and 2230 UT on 9 July, and at about 0915 and 1230 UT on 10 July (Fig. 4). The $3f_g/2$ and $5f_g/2$ emissions occur just above f_g, as determined from the magnetometer instrument (*6*). The upper hybrid emission in the 56-kHz channel at 2230 UT, in the 31-kHz channel at 0915 UT, and in the 17-kHz channel at 1230 UT are very intense, with maximum electric field intensities of 3 to 5 mV m^{-1}. In every case the half-integral harmonic emissions and the upper hybrid emissions occur at the magnetic equator, as determined from the magnetic field data (*6*).

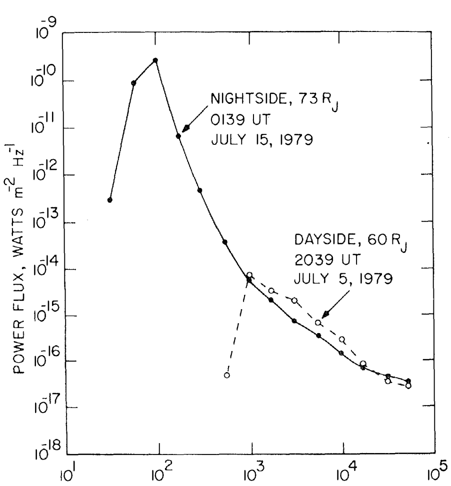

Fig. 6. A comparison of continuum radiation spectra on the dayside and nightside of Jupiter. The only essential difference is the low-frequency cutoff, which is much lower on the nightside.

A preliminary profile of the electron plasma frequency is shown by the dashed line in Fig. 4, which is based on our identification of emissions at f_{UHR}. This profile is intended only as a rough guide for the electron density in the inner magnetosphere, since there are obviously large gaps between the emissions. In most cases the identification of the upper hybrid emission is unmistakable. However, the planetary radio astronomy team identifies another emission near 2230 UT as an upper hybrid resonance emission (*8*). Nevertheless, in our opinion the 56-kHz emission has all of the essential characteristics of the intense upper hybrid emissions observed in Earth's magnetosphere and we believe that this emission is at f_{UHR}.

After passing through the inner regions of the magnetosphere, Voyager 2 provided an extended series of observations in the predawn taillike region of the magnetosphere. The plasma wave observations in this region were dominated by intense broadband emissions extending from as low as 31 Hz to about 10 kHz. These emissions are closely controlled by the rotation of Jupiter. A 3-day period, which clearly illustrates the 10-hour periodicity of these emissions, is shown in Fig. 5. Similar broadband emissions of this type were also detected in the predawn region by Voyager 1, although at that time the interpretation was uncertain (*1*). After studying both the Voyager 1 and 2 observations of this noise, we now believe that the noise consists of electromagnetic continuum radiation in regions of exceedingly low plasma density which occur between encounters with the high-density magnetoplasmadisc (*9*). This interpretation is supported by spectrum comparisons of the continuum radiation in the dayside of the magnetosphere with similar spectra of the broadband emissions in the predawn region. Figure 6, for example, shows two such spectra, one at 2039 UT on 5 July during the inbound pass and the other at 0139 UT on 15 July during the outbound pass. The close similarity of the two spectra is obvious, the only essential difference being the position of the low-frequency cutoff. Because the continuum radiation trapped within the magnetosphere has access to all regions with $f > f_p$ (local), it is not surprising that the high-frequency portions of the spectra should agree, since essentially the same radiation is being detected in both regions.

If the continuum radiation cutoff does extend down to as low as 30 Hz in the predawn region, this cutoff would imply densities as low as 1.0×10^{-5} cm^{-3}. Such low densities on the nightside of Jupiter strongly suggest that the spacecraft is entering a region comparable to the tail lobe of Earth's magnetosphere, which is nearly devoid of plasma. In fact, comparisons of dayside and tail-lobe spectra of continuum radiation in Earth's magnetosphere (*10*) show a strikingly close resemblance to the spectra in Fig. 6, the only essential difference being that the continuum radiation is more intense at Jupiter and extends down to lower frequencies. Although the intense broadband emissions detected on the outbound pass through the tail almost certainly consist of continuum radiation, other narrowband emissions are also known to occur near the low-frequency cutoff of the continuum radiation. At the time of this writing, we have not received sufficient wideband data to adequately investigate the origin of these narrowband emissions.

D. A. GURNETT
W. S. KURTH
Department of Physics and Astronomy, University of Iowa, Iowa City 52242
F. L. SCARF
Space Sciences Department, TRW Defense and Space Systems Group, Redondo Beach, California 90278

References and Notes

1. F. L. Scarf, D. A. Gurnett, W. S. Kurth, *Science* **204**, 991 (1979).
2. F. L. Scarf and D. A. Gurnett, *Space Sci. Rev.* **21**, 289 (1977).
3. W. S. Kurth, D. D. Barbosa, F. L. Scarf, D. A. Gurnett, R. L. Poynter, *Geophys. Res. Lett.* **6**, 747 (1979); J. W. Warwick *et al.*, *Science* **204**, 995 (1979).
4. D. A. Gurnett and R. R. Shaw, *J. Geophys. Res.* **78**, 8136 (1973).
5. D. A. Gurnett, R. R. Anderson, B. T. Tsurutani, E. J. Smith, G. Paschmann, G. Haerendel, S. J. Bame, C. T. Russell, *ibid.*, in press.
6. N. F. Ness *et al.*, *Science* **206**, 966 (1979).
7. K. Rönnmark, H. Borg, P. J. Christiansen, M. P. Gough, D. Jones, *Space Sci. Rev.* **22**, 401 (1978).
8. J. W. Warwick *et al.*, *Science* **206**, 991 (1979).
9. D. D. Barbosa, D. A. Gurnett, W. S. Kurth, F. L. Scarf, *Geophys. Res. Lett.* **6**, 785 (1979).
10. D. A. Gurnett, *J. Geophys. Res.* **80**, 2751 (1975).
11. We express our thanks to the personnel of the Voyager Project Office at the Jet Propulsion Laboratory (JPL) and to the staff of NASA Headquarters for their invaluable support of this investigation. We also thank A. Lane and R. Poynter of JPL for their efforts in improving the wideband coverage and P. Jepsen and G. Garneau for developing the color spectrogram processing. We acknowledge the excellent programming support provided by R. West and R. Brechwald of the University of Iowa. We also thank N. Ness, S. M. Krimigis, H. Bridge, and J. Warwick for providing data in advance of publication and for their helpful discussions. The research at the University of Iowa was supported by NASA through contract 954013 with JPL and through grant NGL-16-001-043 with NASA Headquarters. The research at TRW was supported by NASA through contract 954012 with JPL.

26 September 1979

Planetary Radio Astronomy Observations from Voyager 2 Near Jupiter

Abstract. *The Voyager 2 Planetary Radio Astronomy experiment to Jupiter has confirmed and extended to higher zenomagnetic latitudes results from the identical experiment carried by Voyager 1. The kilometric emissions discovered by Voyager 1 often extended to 1 megahertz or higher on Voyager 2 and often consisted of negatively or, less frequently, positively drifting narrowband bursts. On the basis of tentative identification of plasma wave emissions similar to those detected by Voyager 1, the plasma torus associated with Io appeared somewhat denser to Voyager 2 than it did to Voyager 1. We report here on quasiperiodic sinusoidal or impulsive bursts in the broadcast band range of wavelengths (800 to 1800 kilohertz). A Faraday effect appears at decametric frequencies, which probably results from propagation of the radiation near its sources on Jupiter. Finally, we discuss the occurrence of decametric emission in homologous arc families.*

On 9 July 1979, Voyager 2 carried the second low-frequency radio receiver (*1*) to be flown into Jupiter's environment. The experiment was virtually identical to that carried past Jupiter by Voyager 1 (*2*) on 5 March 1979, notable differences being the higher zenomagnetic latitudes of the approach trajectory, and the more distant encounter with Jupiter of Voyager 2. Our purpose here is, once again, to present selected results related to these differences and to some of the many phenomena we could only mention in the earlier report (*2*).

As our familiarity with radio Jupiter has grown in the months since the Voyager 1 encounter, we have found it necessary to review some of our preliminary ideas, especially with respect to the source or sources of the kilometric wavelength (KOM) radiation. We concluded (*2*) that the coincidence of the observed wave frequencies of KOM with the plasma frequencies observed in the Io torus provided an argument in favor of the torus as the source of KOM. We have often seen on Voyager 1 and 2 instances of "KOM" radiation extending to much higher frequencies than the 500 kHz of a typical event, often to 1 MHz and above. As we shall see, the Io torus was probably more dense than at the time of the Voyager 1 encounter, although it is not clear whether the increased torus density can support radiation as high as 1 MHz. Furthermore, at

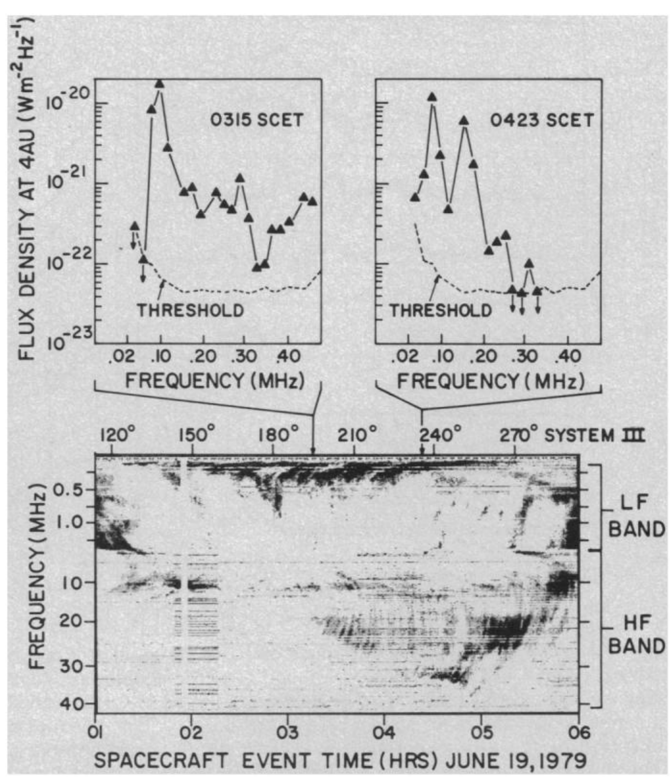

Fig. 1. Dynamic spectrum of Jupiter's radio emissions observed by the Planetary Radio Astronomy (PRA) instrument on Voyager 2. The total received power in each of the 198 frequency channels is shown as a function of spacecraft event time (*SCET*) and sub-Voyager Jupiter longitude [system III (1965)]. Increasing power is indicated by increasing darkness. The PRA receiver is divided into (i) a 70-channel, low-frequency (*LF*) band between 1.2 kHz and 1.3 MHz with a 1-kHz bandwidth and (ii) a 128-channel, high-frequency (*HF*) band between 1.2 MHz and 40.5 MHz with a 200-kHz bandwidth. Between 0130 and 0500 SCET, a KOM event can be seen in the LF band extending from 0.04 to nearly 1 MHz. It is composed of numerous narrowband drifting structures. In the upper two panels, flux density spectra are shown at two different times, illustrating the intensity behavior of the KOM emission. In the HF band, an Io-A or main-"source" event with characteristic arc structure can be seen centered on 240° longitude.

0036-8075/79/1123-0991$01.00/0